RSC Advances

ROYAL SOCIETY OF CHEMISTRY

www.rsc.org/advances

Cite this: DOI: 10.1039/c0xx00000x

www.rsc.org/xxxxxx

Full Paper

New conjugated poly(pyridinium salt) derivative: AIE characteristics, the interaction with DNA and selective fluorescence enhancement induced by dsDNA

Ying Chang, Lu Jin, Jingjing Duan, Qiang Zhang, Jing Wang and Yan Lu*

Received (in XXX, XXX) Xth XXXXXXXXX 20XX, Accepted Xth XXXXXXXXX 20XX
DOI: 10.1039/b000000x

Herein, a new conjugated poly(pyridinium salt) derivative **L** was synthesized by the ring-transmutation polymerization reaction for the purpose of sensitive and selective fluorescence sensing of DNA. Cationic **L** exhibits aggregation-induced emission (AIE) characteristics that is weakly emissive in solution but highly luminescent in the aggregate state. Based on its AIE activity, a fluorescence turn-on biosensor for calf thymus DNA (*ct*DNA) detection is developed, which shows excellent selectivity with a detection limit down to the 10^{-8} M^{-1} in CH_3CN-phosphate buffer solution (PBS) (2 mM, pH 7.4) (v/v 1:1). Further, the interactions between **L** and *ct*DNA are carefully investigated by UV-vis absorption spectra, dynamic light scattering (DLS) measurements, thermal denaturation studies, circular dichroism (CD) measurements, as well as competing experiments with ethidium bromide (EB). More interestingly, **L** exhibits selective fluorescence enhancement induced by double-stranded DNA (dsDNA), therefore, **L** was also successfully utilized as fluorescent probe to follow the *ct*DNA cleavage process by bovine pancreatic deoxyribonuclease I (DNase I).

Introduction

Fluorescent biosensors for DNA detection have received great attention because of their ultrasensitivity and rapid and easy operations, and accordingly, they show widespread applications in gene expression profiling, clinical disease diagnostics, and the drug industry.[1] Conjugated polyelectrolytes (CPEs) integrate the optoelectronic properties of conjugated polymers with the electrostatic behavior of polyelectrolytes, providing a unique platform for the construction DNA biosensors.[2] Thanks to the enthusiastic efforts of scientists, a variety of CPEs such as polyfluorene, polyarylene and polythiophene derivatives have been developed for sensing of a wide range of DNA-related events.[2] Most of them involved in the fluorescence resonance energy transfer (FRET) from cationic polyfluorenes to fluorescein-labeled DNA. This entails the cost, complexity, and time required. Moreover, it is not favorable for practical use that the fluorescence of polyfluorenes is quenched by DNA.[3] Recently, a breakthrough in the synthesis of fluorescent organic dyes, with intriguing aggregation-induced emission (AIE) phenomena, offers a new platform for developing new sensing systems that operate in a "turn-on" mode.[4] These AIE-active dyes are weakly fluorescent in solution but become highly fluorescent upon aggregation induced by analytes. For example, Tang et al. developed a versatile AIE probes for nucleic acid detection and quantitation.[5] Liu et al. reported a simple singly labelled DNA probe with AIE characteristics for specific DNA hybridization detection.[6] However, AIE luminogen (AIEgen) reported is relatively limited so far, which mainly includes hexaphenylsilole (HPS), tetraphenylethene (TPE) and their derivatives. So, creation of new fluorogenic CPEs with AIE attributes is still required for the development of new sensing system with high sensitive and selectivity.

We have been devoting ourselves to develop a new kind of CPEs based on poly(pyridinium salt)s derivatives for bio-related molecules sensing.[7] Unlike most of CPEs-based fluorescent probes which are characterized by a backbone with a delocalized electronic structure and the charged functional side chains, poly(pyridinium salt)s derivatives belong to a class of main-chain polyelectrolytes, consist of 4,4'-(1,4-phenylene)bis(2,6-diphenylpyridinium) ions along the backbone. Besides good thermo-stability as well as abundant and tunable photoelectric properties,[8] the charged nature of their main-chains also permits coordination of electrostatic forces with oppositely charged analyte targets. Recently, we reported an alternative conjugated poly(pyridinium salt)s containing carbazole in the main chain, which exhibited AIE characteristics and have been used as fluorescent turn-on DNA sensors by taking advantage of complexation-induced aggregation through electrostatic attration between poly(pyridinium salt)s and DNA.[7c]

Herein, we report a new conjugated poly(pyridinium salt) derivative (**L**) with AIE characteristics for fluorescence turn-on detection of DNA based on complexation-induced aggregation by the synergistic electrostatic attration and intercalating interaction. **L** exhibits selective fluorescence enhancement induced by double-stranded DNA (dsDNA), therefore, **L** is also successfully employed to follow the DNA cleavage process by nuclease.

Experimental section

Materials

All chemical reagents were obtained commercially and used as received unless otherwise stated. Calf thymus DNA (*ct*DNA) was purchased from Beijing Sunbiotech Co. Ltd, and purified by phenol extraction until UV absorbance 260nm/ 280nm was > 1.9. The DNA concentration per nucleotide was determined by absorption spectroscopy by using the molar absorption coefficient (ε = 6600 mol^{-1} m^3 cm^{-1}) at 260 nm. Bovine pancreatic deoxyribonuclease I (DNase I) and single-stranded DNA (ssDNA) are purchased from Sigma Co. ssDNA with 24 bases: 5'-GGTGGCCATTACCTTTGACTCTTC-3' ($ssDNA_1$), ssDNA with 34 bases: 5'-CCACCTGTTGGTAGTCCTTGTATTTAGT-ATCATC-3') ($ssDNA_2$). Milli-Q water (18.2 MΩ) was used for all the experiments. Phosphate buffer solution (PBS) was purchased from Beijing Dingguo Biotechnology Co. Ltd.

General characterization

^{1}H and ^{13}C NMR spectra were measured on a Varian UNITY Plus-400 NMR spectrometer (400 MHz) using tetramethylsilane (TMS) as an internal reference for NMR analyses. The element analysis was performed on a Perkin-Elmer 2400C instrument. GPC analysis was conducted with a Waters 2690 liquid chromatography system equipped with Waters 996 photodiode detector and Phenogel GPC columns, using polymethyl methacrylate as the standard and DMF as the eluent at a flow rate of 1.0 mL/min at 35°C. A 50 μL of 0.2 wt% of polymer in DMF containing 0.01M LiBr was injected in the columns. The pH measurements were carried out on a Mettler-Toledo Delta 320 pH meter. UV-vis absorption spectra were recorded on a Shimadzu UV-2550 spectrometer. Fluorescence spectra were measured on a Hitachi F-4600 fluorescence spectrophotometer equipped with a xenon lamp excitation source. All circular dichroism (CD) spectra were measured on a Jasco J-715 WI spectropolarimeter using a cylindrical quartz cell with a pathlength of 10 mm. All the spectrum measurements were performed at 25 °C. Dynamic light scattering (DLS) measurements were performed using a Zetasizer Nano ZS90 (Malvern Instruments Co., UK) equipped with a He-Ne laser.

Synthesis of 4-nitrotriphenylamine (1)

Compounds **1** were synthesized from a procedure described in the literature.[9] m.p. 144 -145 °C; ^{1}H NMR (400 MHz, d_6-DMSO, ppm): δ 8.08 (m, 2H), 7.47 (m, 4H), 7.29 (ddd, J = 8.5, 7.4, 3.0 Hz, 6H), 6.81 (m, 2H).

Synthesis of 4-aminotriphenylamine (2)

Compounds **2** were prepared according to the known procedure.[10] m.p. 148-149 °C; ^{1}H NMR (400 MHz, d_6-DMSO, ppm): δ 7.13 (dd, J = 20.6, 13.0 Hz, 6H), 6.90 (m, 8H), 6.58 (s, 2H).

Synthesis of N,N-bis(4-nitrophenyl)-N′,N′-diphenyl-1,4-phenylenediamine (3)

Compounds **3** were synthesized according to the reported method.[11] m.p. 219-220 °C; ^{1}H NMR (400 MHz, d_6-DMSO, ppm): δ 8.20 (m, 4H), 7.33 (tt, J = 3.9, 2.0 Hz, 4H), 7.21 (m, 2H), 7.19 (t, J = 2.0 Hz, 4H), 7.17 (d, J = 0.9 Hz, 2H), 7.10 (ddd, J = 7.0, 5.0, 2.7 Hz, 4H), 7.01 (m, 2H).

Synthesis of N,N-bis(4-aminophenyl)-N′,N′-diphenyl-1,4-phenylenediamine (4)

Compound **4** were synthesized from a similar procedure described in the literature.[12] Compound **3** (1.02 g, 2.03 mol), Pd/C catalyst (23 mg, 0.2 mmol) and hydrazine monohydrate (1.0 mL) were mixed in 25 mL of ethanol, and stirred at reflux for 7h at 95 °C. After cooling, the resulting precipitate was dissolved in THF (50 mL). The solution was filtrated to remove Pd/C, filtrate was distilled until the solvent evaporated. The crude product was washed with methanol and recrystallized from acetonitrile in nitrogen, and then dried under reduced pressure to give light-beige compound **4** (0.70 g, 78%). m.p. 241-242 °C; ^{1}H NMR (400 MHz, d_6-DMSO, ppm): δ 7.23 (t, J = 7.8 Hz, 4H), 6.92 (t, J = 7.0 Hz, 6H), 6.83 (d, J = 7.9 Hz, 6H), 6.59 (d, J = 8.5 Hz, 2H), 6.54 (d, J = 8.4 Hz, 4H), 4.97 (s, 4H). ^{13}C NMR (100 MHz, d_6-DMSO, ppm): δ 148.16, 147.70-146.57 (m), 146.03, 138.74-136.99 (m), 136.76-135.36 (m), 129.52, 127.76, 122.18, 118.11, 115.31.

Synthesis of 4,4'-(1,4-phenylene)bis(2,6-diphen-yl-pyrylium) ditosylate (5)

Compounds **5** were synthesized according to our previous work with 75 % yield as orange powder.[7] ^{1}H NMR (400 MHz, d_6-DMSO, ppm): δ 9.36 (s, 4H), 9.16 (s, 4H), 7.59-8.93 (m, 20H),7.47 (d, J = 6.7 Hz, 4H), 7.10 (d, J = 7.7 Hz, 4H), 2.27 (s, 6H). ^{13}C NMR (100 MHz, d_6-DMSO, ppm): δ 146.12, 138.11, 132.38-127.49 (m), 125.96, 39.96, 21.39.

Polymer synthesis

The synthesis pathway of polymer was shown in Scheme 1. A solution of monomer **4** (0.33 g, 0.75 mmol) and another monomer **5** (0.67 g, 0.75 mmol) in 20 mL of DMSO was vigorously stirred and heated at 110 °C under nitrogen for 2 h. Toluene (10 mL) was then added so that the water generated by the transformation of the pyrylium ring to the pyridinium ring could be removed as a toluene/water azeotrope. Then, the bath temperature was increased to 150 °C and the azeotrope and the excess toluene were gradually distilled from the reaction mixture using a Dean–Stark trap over 4-5 h. The bath temperature was maintained at that temperature for 48 h. the resulting viscous solution was slowly poured into a large excess (25 times in volume) of rapidly stirred ethyl acetate. The precipitate was collected by filtration, washed with water and dried under reduced pressure at 120 °C overnight to give polymer **L** (0.90 g, 90%). ^{1}H NMR (400 MHz, d_6-DMSO, ppm): δ 8.86 (s, 4H), 8.66 (s, 4H), 7.37 (m, 32H), 7.03 (m, 12H), 6.50 (s, 6H), 2.26 (s, 6H). ^{13}C NMR (101 MHz, d_6-DMSO, ppm): δ 157.11, 146.91, 137.97, 133.55, 131.64-127.36 (m), 126.81-121.20 (m), 40.02, 21.25. IR (KBr, cm^{-1}): 3051.38 (=C-H aromatic stretching), 1594.62-1452.89 (C=C and C=H aromatic ring stretching), 1222.8 ($C-N^+$), 1119.55 (S=O asymmetric stretching), 1032.55-1011.82 (symmetric stretching), 846.24-679.01 (=C-H out-of-plane bending). Anal. calcd for $C_{84}H_{64}N_4O_6S_2$: C, 78.17; H, 5.08; N, 4.34. Found: C, 78.21; H, 5.35; N, 4.41%. M_n = 40 617, polydispersity induces (PDI) = 1.44.

Results and discussion

Polymer synthesis and characterization

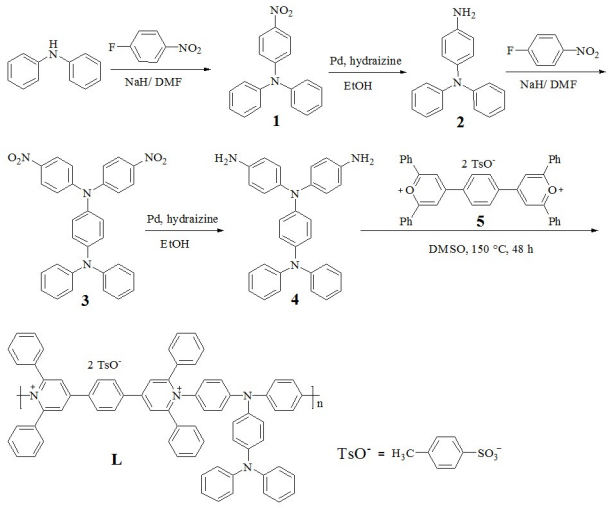

Scheme 1 Synthesis route for conjugated poly(pyridinium salt) **L**.

Scheme 1 outlines the reaction sequence applied for the synthesis of probe **L**. The new conjugated poly(pyridinium salt)s **L** were prepared by the ring-transmutation polymerization reaction that was carried out on heating in DMSO as previously reported.[7, 8] The chemical structure of **L** are consistent with the spectra of FTIR, ^{1}H and ^{13}C NMR spectroscopy, and elemental analysis. The number-average molecular weight and polydispersity of **L** were 40 617 and 1.44 respectively, determined by gel-permeation chromatography (GPC) using DMF containing 0.01M LiBr as the solvent, and polymethyl methacrylate as standards. The detailed information is also presented in ESI.

AIE properties of polymer

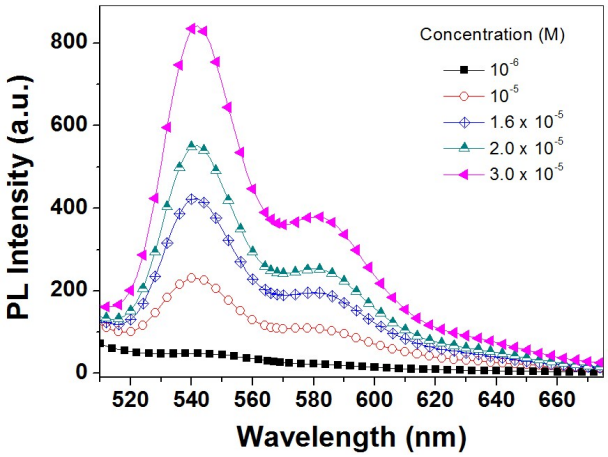

Fig. 1 Photoluminescent spectra of **L** in CH_3CN-H_2O (v/v =1:1) of various concentrations. (excited at 430 nm).

Effect of concentration was emphasized by the unnormalized PL emission spectra as shown in Fig. 1, which exhibited the continuous accession of the emission intensity with increasing concentration. Whereas solution thickening often quenches light fluorophore's emission, **L** solutions become more emissive with higher concentration. This peculiar phenomenon of concentration-enhanced emission is possibly due to the AIE effect, as we will discuss later. Here, solution (10^{-6} M) with very low fluorophore content is essentially weak in emission, but upon increasing the concentration of **L** to 10^{-5} M range, two overlapping emission bands started to emerge and to have enhanced emission magnitudes with increasing concentration. The short- and longwavelength emissions are supposed to be due to the **L** itself and the aggregation emissions, respectively.[13]

The AIE effect can also be characterized by examining the emission behavior of **L** in solvent mixtures with different fractions of CH_3CN and water (Fig. S12, ESI). Since water is nonsolvent for **L**, the hydrophobic polymer chains of **L** are considered to form aggregates in the CH_3CN/water mixtures. Mixtures of **L** in CH_3CN/water were vigorously stirred to ensure uniform dispersion of the polymer aggregates before emission measurements. All the resultant mixture solutions (5 μM, relative to repeat unit) are macroscopically homogeneous with no precipitate up to water fraction of 50 vol % water, and upon further increasing the water fraction, the solution becomes visually opaque. These results indicate the formation of aggregate upon the addition of water. As shown in Fig. S12, upon excitation at 430 nm, the solution (5 μM) of **L** in pure CH_3CN emitted weakly, and with the increasing amount of water added, the corresponding mixture solution exhibited a obvious increase in the emission intensity. For the 50 vol% water solution, about 3.5-fold emission enhancement along with a red-shift of emission peak from 528 nm to 541 nm was observed compared to **L** in pure CH_3CN. These data indicate that the fluorescence of **L** tends to be enhanced by aggregation, which may be attributed to the restrictions of intramolecular rotations of conjugated backbone of **L** in the aggregate state.[14]

Since cooling can also fortify the RIR process, we studied the temperature effect on **L** emission to further confirm the AIE activity of **L**. DMF is used in the study because of its strong solvating power and low melting point (– 61 °C), which can help keep the solution molecules in the solution state at low temperatures. When a DMF solution of **L** is cooled, its emission intensity is increased as shown in the Fig. S13 (ESI), which should be attributed to the molecular rotation are greatly restrained at lower temperature.

UV-vis absorption spectra response to *ct*DNA addition

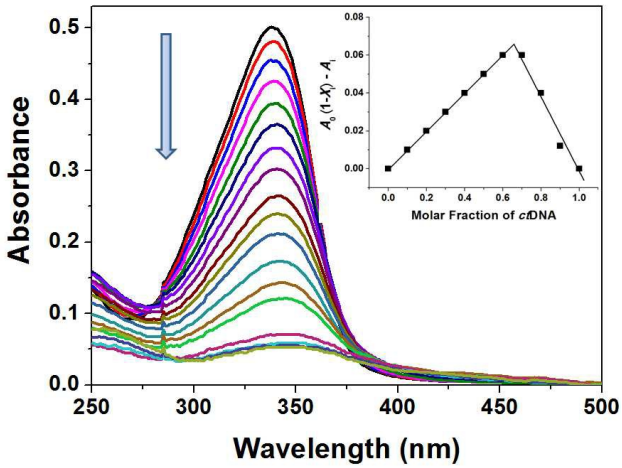

Fig. 2 UV-vis absorption spectra of **L** ([**L**] = 5 μM) in the presence of different concentrations of *ct*DNA in CH_3CN-H_2O (v/v =1:1). [*ct*DNA] = 0, 1.25, 2, 3, 4.25, 5, 5.5, 5.7, 5.9, 6.0, 6.1, 6.2, 6.3, 6.4, 6.5, 7.5, 9.5, 11.0 μM. Inset: Job's plot. A_0 is the initial absorbance of the free **L**, A_i is the recorded absorbance of complexes at different *ct*DNA concentrations in CH_3CN-H_2O (v/v =1:1), and X_i is the molar fraction of *ct*DNA.

The interaction between **L** and *ct*DNA was firstly performed by exploring the UV-vis spectra changes of **L** when titrated with *ct*DNA. Since **L** are cationic conjugated polyelectrolytes, whereas *ct*DNA carries highly electronegative charges on the phosphate groups, they can form complexes through electrostatic attraction. As shown in Fig. 2, **L** exhibits a maximal absorption at 337 nm (ε = 1.0 × 10^5 M^{-1} cm^{-1}), which is associated to the π–π^* transition of the conjugated polymer **L** backbone. With the increment of *ct*DNA, the absorbance at 337 nm of **L** decreased gradually, which was concomitant with red-shift of maximal absorption peak by about 10 nm, signifying significant aggregate between the **L** and *ct*DNA was formed.

Job's plot yielded from UV-vis absorption shows a nearly 1:2 stoichiometry for the complexes of **L** with *ct*DNA (see inset in Fig. 2). The binding constants of **L**-*ct*DNA complexes is estimated to be 1.07×10^5 M^{-1} according to the reported method.[15]

DLS analysis of the L complexes with *ct*DNA

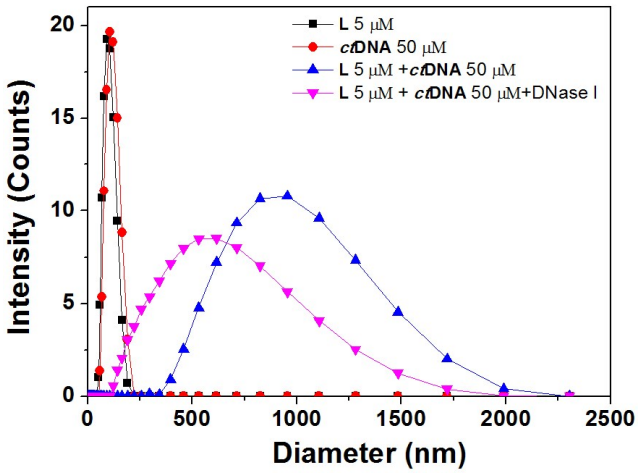

Fig. 3 Hydrodynamic diameter of **L** (5 μM) in the presence of *ct*DNA and DNase I in an CH_3CN-H_2O (v/v =1:1) obtained from DLS.

To probe the polymer aggregation in acetonitrile aqueous solution, DLS experiments were performed and shown in Fig. 3. **L** formed small aggregates with a mean diameter of about 90 nm, which is ascribed to its poor water solubility. Upon the addition of *ct*DNA, the hydrodynamic diameter of the aggregates increased significantly. The mean diameter is of about 890 nm at [*ct*DNA] = 50 μM. Thus, near the endpoint of the UV spectra titration, **L**-*ct*DNA complexes exist in a highly aggregated state.

Competing experiments with EB

It is well known that EB can intercalates within the internally stacked bases of dsDNA, resulting in an increase in its fluorescence intensity.[16] To explore whether **L** binds to *ct*DNA by intercalative interaction, the competing experiments of **L** with EB was performed. Upon addition of 10 equiv of *ct*DNA to the solutions of EB, an increase of the florescent emission positioned at 623 nm with an enhancement factor of 14.7-fold was observed as shown in Fig. S14 (ESI). Then adding **L** to an equilibrated EB-*ct*DNA solution, resulted in the decrease of emission intensity of EB at 623 nm. The results indicated that probe **L** can weakly intercalative binding to duplex *ct*DNA.

Thermal denaturation studies

To further examine binding mode of **L** with *ct*DNA, UV-melting transition were measured and shown in Fig. S15 (ESI). The *ct*DNA melting temperature (T_m), *i.e.*, the temperature at which a double-to-single strand transition happens and are determined by monitoring the absorption of DNA at 260 nm reaches 50% of the maximal value in the presence and absence of **L**. Fig. S15 exhibits an increase in the melting point by 8 °C in the presence of **L**, which indicates that polymer **L** binding to *ct*DNA stabilized the double helix. The significant increase of T_m demonstrates that **L** can intercalate abilities into the double helical DNA.[17]

Circular dichroism measurements

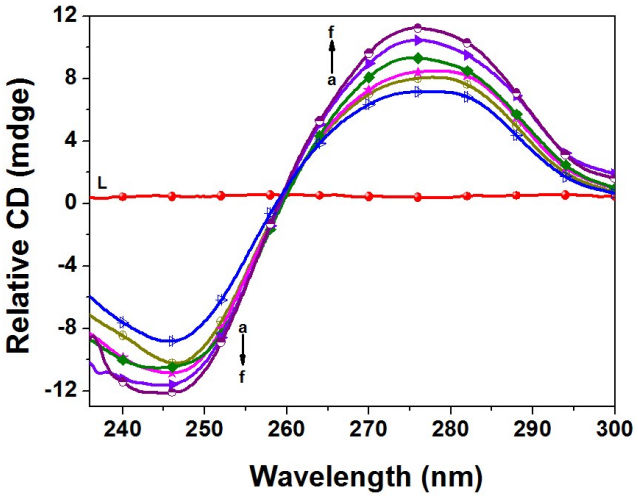

Fig. 4 Circular dichroism spectra of *ct*DNA (60 μM) in CH_3CN-H_2O (v/v = 1:1) upon addition of polymer **L**. [**L**] = 0, 8, 12, 16, 22 and 24 μM from *a* to *f*, respectively.

In order to check whether the *ct*DNA structure changes upon binding to cationic polymer **L**, CD measurements of *ct*DNA were performed in the presence and absence of **L** in CH_3CN-H_2O (v/v 1:1) (Fig. 4). As shown in Fig. 4, the intrinsic CD activity of the **L** was recorded and found to be negligible. In the absence of **L**, the CD spectrum of *ct*DNA was of typical B-form, which exhibited a positive Cotton effect at about 275 nm due to base stacking and a negative Cotton effect at about 245 nm attributed to the right-handed helicity of *ct*DNA.[18] Upon addition of polymer **L**, the intensites of both the negative peak at 245 nm and the positive peak at 275 nm in the CD spectra increased as the concentration of **L** was increased from 0 to 24 μM, indicating an significant change in conformation of the *ct*DNA structure as **L** binds to the duplex.

Changes in the intensity of the CD peak at 245 nm have been associated with alteration of hydration of the helix in the vicinity of phosphate or the ribose ring as the ionic concentration is altered.[19] Therefore, it would be reasonable to suggest that exchanging a cationic polymer **L**, with sodium ion would lead to changes in hydration near the phosphate group of the DNA helix. While the changes in the intensity of the CD peak at 275 nm should be attributed to the intercalation interaction between the phenyl groups on the side chain of polymer **L** and the *ct*DNA base pairs *via* hydrophobic force as demonstrated by competing experiments with EB. Thus, the synergetic electrostatic attraction and intercalation interaction should be responsible for the binding of *ct*DNA with **L**.

Complexation-enhanced fluorescence

Fig. 5 shows the fluorescence spectra of **L** ([**L**] = 5 μM) and those in the presence of different concentration of *ct*DNA in CH_3CN-PBS (2 mM, pH 7.4) (v/v 1:1). As shown in Fig. 5, **L** was weakly emissive in solution with maximum emission peak at 541 nm. However, upon addition of *ct*DNA to the solution of **L**, the fluorescence intensity at 541 nm enhanced sharply to 10.2 times its individual intensity in the absence of *ct*DNA, then tended to saturation when the *ct*DNA concentration reached 23.6 μM. At the saturation point, the negative charges from DNA are more than positive charges from **L**, thus, aggregation of polymer **L** occurs around *ct*DNA should be formed, which restricts the structure torsional of **L**, thereby, reducing energy consumption and enhancing the fluorescent intensity.

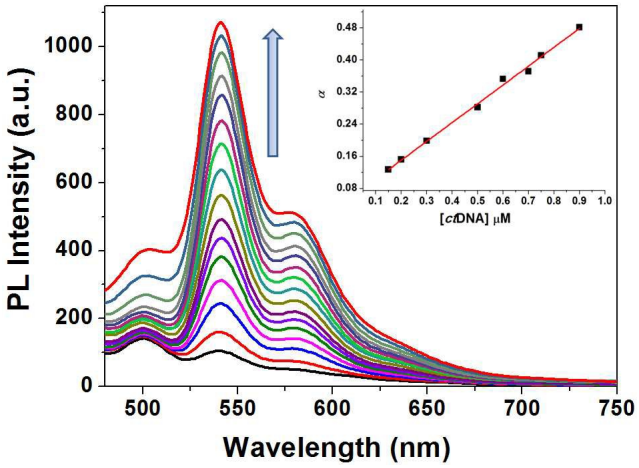

Fig. 5 Fluorescent titration spectra of **L** (5 μM) in CH_3CN-PBS (2 mM, pH 7.4) (v/v 1:1) in the presence of *ct*DNA at different concentrations ranging from 0 to 23.6 μM (λ_{ex} = 430 nm). Inset: α as a function of [*ct*DNA] at low *ct*DNA concentration. The data are based on the average of four independent experiments.

In order to determine the detection limit of probe **L** for *ct*DNA, lower *ct*DNA concentration ranging from 0.15 to 0.90 μM were studied by fixing concentration of **L** at 5 μM and then adding aliquots of stock solution of *ct*DNA. We define α as: $\alpha = (F - F_0) / F_0$, where F and F_0 are the intensities at 541 nm in the presence and absence of *ct*DNA, respectively. Inset (Fig. 5) shows α as a function of *ct*DNA concentration. A linear regression curve was obtained with a correlation coefficient of 0.995. The point at which this line crossed the horizontal axis was taken as the detection limit and equaled approximately 3.2×10^{-8} M^{-1} free *ct*DNA in CH_3CN-PBS (2 mM, pH 7.4) (v/v 1:1).[20] The slope is 0.469 μM^{-1}, indicating the high sensitivity of **L** to *ct*DNA, which is consistent with the strong complexation of **L** to *ct*DNA.

Selectivity

To investigate the selectivity of probe **L**, various anions sodium salts as well as two ssDNA with different base length have been added to **L** solutions. As shown in Fig. 6 and Fig. S16 (ESI), after addition of 5 equiv amount of these anions to solutions of **L**, the solutions did not lead to significant fluorescence increase. The good selectivity for *ct*DNA is associated with synergetic electrostatic attraction and intercalation interaction between *ct*DNA and **L**, which consequently induces enhanced fluorescence emission by AIE effect. This results suggests that **L** can be used as a selective fluorescent probe for *ct*DNA in the presence of other types of ssDNA and other various anions which can compete with *ct*DNA to bind with **L**.

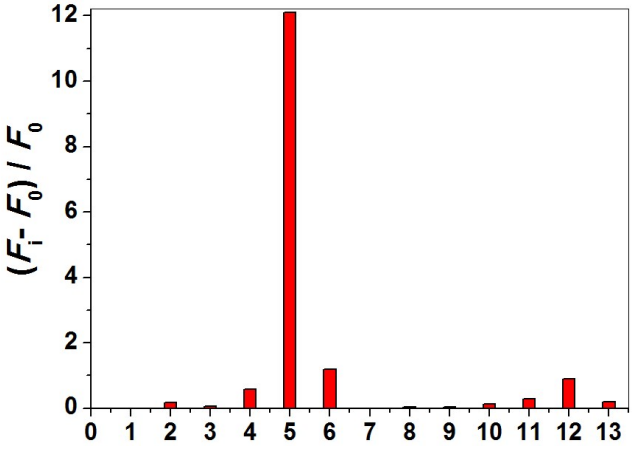

Fig. 6 Change in the ratio ((F_i - F_0)/ F_0) of fluorescence intensity of **L** (5 μM) in CH_3CN-H_2O (v/v 1:1) in the presence of 5 equiv of various anions. F_i and F_0 are the intensities at 541 nm in the presence and absence of different anions, respectively. 1: **L**; 2: **L** + Cl^-; 3: **L** + Br^-; 4: **L** + $ssDNA_1$; 5: **L** + *ct*DNA; 6: **L** + $ssDNA_2$; 7; **L** + HCO_3^-; 8: **L** + HPO_4^{2-}; 9: **L** + HSO_4^-; 10: **L** + I^-; 11: **L** + $P_2O_7^{4-}$; 12: **L** + PO_4^{3-}; 13: **L** + SO_4^{2-} (λ_{ex} = 430 nm).

Label-free fluorescence nuclease assay

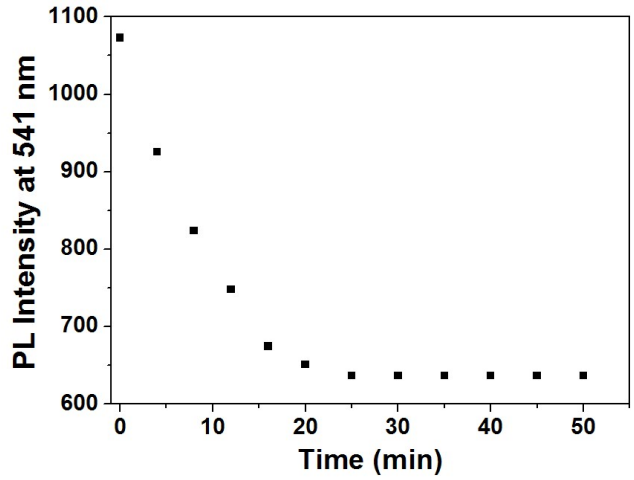

Fig. 7 Plot of fluorescence intensity at 541 nm of **L** (5 μM) in CH_3CN-PBS (2 mM, pH 7.4) (v/v 1:1) against time in the presence of 10 equiv of *ct*DNA upon addition of 3 equiv DNase I.

DNA cleavage reactions catalyzed by various enzymes such as restriction nuclease and nonspecific nuclease are very important in biological processes involving the replication, repair, and recombination of DNA.[21] In the present work, bovine pancreatic deoxyribonuclease I (DNase I), which is an endonuclease that preferentially splits phosphodiester linkages adjacent to a pyrimidine nucleotide, yielding 5'-phosphate terminated polynucleotides with a free hydroxyl group at the 3' position, is employed to demonstrate the potential application of **L** as a fluorescent probe to follow the DNA cleavage process by nuclease. Furthermore, such label-free fluorescence nuclease assay could be used for nuclease inhibitor screening.

Before the reaction of *ct*DNA with DNase I, the ensemble of **L** and *ct*DNA exhibited rather strong fluorescence as shown in Fig. 7. But, the fluorescence of the ensemble of was gradually reduced after *ct*DNA hydrolyzed by DNase I with prolonging the reaction time. It should be pointed out that the fluorescence enhancement of **L** after mixing DNase I under the same conditions can be neglected. With the DNA cleavage by DNase I, the aggregation of **L** becomes less efficient, as a result, the mean hydrodynamic diameter decreases to 560 nm as shown in Fig. 3. The preliminary results indicate the potential application of **L** as a fluorescent probe to develop a label-free fluorescence nuclease assay.

Conclusions

In summary, a new fluorescent poly(pyridinium salt) derivative **L** was synthesized *via* the ring-transmutation polymerization reaction. **L** exhibits interesting AIE activity, providing a new sensing platform for biomolecules detection. The interactions between **L** and *ct*DNA were carefully investigated by UV-vis absorption spectra, DLS measurements, thermal denaturation studies, CD measurements, as well as competing experiments with EB. These results indicate the synergetic electrostatic attraction and intercalation interaction should be responsible for the binding of *ct*DNA with **L**. Furthermore, fluorescence turn-on DNA biosensor with high sensitivity and selectivity was developed by taking advantage of AIE effect of **L**. **L** was then utilized successfully as fluorescent probe to follow the DNA cleavage process by nuclease. With smart structural design, we anticipate that this type of polymers has ideal properties to be used as fluorescence turn-on biosensors for detection of other bio-related molecules.

Acknowledgements

This work was financially supported by the National Natural Science Foundation of China (NO: 21074093, 20972111) and the Program for New Century Excellent Talents in University (NCET-12-1066).

Notes and references

Tianjin Key Laboratory for Photoelectric Materials and Devices, School of Materials Science & Engineering, Tianjin University of Technology, Tianjin 300384, China.
Fax: +86-22-60214500; Tel: +86-22-60216748; E-mail: luyan@tjut.edu.cn

† Electronic Supplementary Information (ESI) available: [Synthesis and characterization data of compounds **1-5**; Calt thymus DNA melting curves in the absence and presence of **Poly1**; PL spectra of **Poly1** in PBS solution in the presence of different concentrations of calf thymus DNA]. See DOI: 10.1039/b000000x/

1 (a) H. A. Ho, A. Naiari and M. Leclerc, *Acc. Chem. Res.*, 2008, **41**, 168; (b) S. W. Thomas, G. D. Joly and T. M. Swager, *Chem. Rev.*, 2007, **107**, 1339; (c) C. Debouck and P. N. Goodfellow, *Nat. Genet.*, 1999, **21**, 48; (d) M. J. Heller, *Annu. Rev. Biomed. Eng.*, 2002, **4**, 129.

2 (a) C. Chi, A. Mikhailovsky and G. C. Bazan, *J. Am. Chem. Soc.*, 2007, *129*, 11134; (b) B. Liu and G. C. Bazan, *Chem. Asian J.*, 2007, **2**, 499; (c) B. S. Gaylord, A. J. Heeger and G. C. Bazan, *J. Am. Chem. Soc.*, 2003, **125**, 896; (d) M. Yu, Y. Tang, F. He, S. Wang, D. Zheng, Y. Li and D. Zhu, *Macromol. Rapid Commun.*, 2006, **27**, 1739; (e) X. F. Liu, Q. L. Fan and W. Huang, *Biosens. Bioelectron.*, 2011, **26**, 2154; (f) W. Lv, N. Li, Y. Li and A. Xia, *J. Am. Chem. Soc.*, 2006, **128**, 10281; (g) K. Lee, L. K. Povlich and J. Kim, *Adv. Funct. Mater.*, 2007, 17, 2580; (h) B. Liu and G. C. Bazan , *Chem. Mater.*, 2004, **16**, 4467; (i) W. J. Zhang, L. Xu, J. G. Qin and C. L. Yang, *Macromol. Rapid Commun.*, 2013, **34**, 442; (j) C. L. Zhu, L. B. Liu, Q. Yang, F. T. Lv and S. Wang, *Chem. Rev.*, 2012, **112**, 4687.

3 (a) S. Wang, B. Liu, B. S. Gaylord and G. C. Bazan, *Adv. Funct. Mater.*, 2003, **13**, 463; (b) H.-A. Ho, M. Boissinot, M. G. Bergeron, G. Corbeil, K. Doré, D. Boudreau and M. Leclerc, *Angew. Chem. Int. Ed.*, 2002, **41**, 1548.

4 (a) J. Luo, Z. Xie, J. W. Y. Lam, L. Cheng, H. Chen, C. Qiu, H. S. Kwok, X. Zhan, Y. Liu, D. Zhu and B. Z. Tang, *Chem. Commun.*, 2001, 1740; (b) R. T. K. Kwok, C. W. T. Leung, J. W. Y. Lamab and B. Z. Tang, *Chem. Soc. Rev.*, 2015, **44**, 4228.

5 Y. Hong, H. Xiong, J. W. Y. Lam, M. Häußler, J. Liu, Y. Yu, Y. Zhong, H. H. Y. Sung, I. D. Williams, K. S. Wong and B. Z. Tang, *Chem.-Eur. J.*, 2010, **16**, 1232; (b) Y. Hong, S. Chen, C. W. T. Leung, J. W. Y. Lam and B. Z. Tang, *Chem.-Asian J.*, 2013, **8**, 1806.

6 Y. Li, R. T. K. Kwok, B. Z. Tang and B. Liu, *RSC Adv.*, 2013, **3**, 10135.

7 (a) Y. Lu, C. C. Xiao, Z. F. Yu, X. S. Zeng,Y. Ren and C. X. Li, *J. Mater. Chem.*, 2009, **19**, 8796; (b) F. L. Han, Y. Lu, Q. Zhang, J. F. Sun, X. S. Zeng and C. X. Li, *J. Mater. Chem.*, 2012, **22**, 4106; (c) J. F. Sun, Y. Lu, D. D. Cheng, Y. J. Sun and X. S. Zeng, *Polym. Chem.*, 2013, **4**, 4045; (d) L. Wang, Y. D. Li, J. F. Sun, Y. Lu, Y. J. Sun, D. D. Cheng and C. X. Li, *J. Appl. Polym. Sci.*, 2014, **131**, 40933; (e) Y. J. Sun, J. Wang, L. Jin, Y. Chang, J. J. Duan, Y. Lu, *Polym. J.*, 2015, DOI: 10.1038/pj.2015.62.

8 P. K. Bhowmik, H. Han, J. J. Cebe, I. K. Nedeltchev, S. W. Kang and S. Kumar, *Macromolecules*, 2004, **37**, 2688; (b) P. K. Bhowmik, S. Kamatam, H. Han and A. K. Nedeltchev, *Polymer*, 2008, **49**, 1748; (c) P. K. Bhowmik, H. Han, and A. K. Nedeltchev, *Polymer*, 2006, **47**, 8281.

9 R. Gujadhur, D. Venkataraman and J. T. Kintigh, *Tetrahedron Lett.*, 2001, **42**, 4791.

10 S. Urgaonkar, J. H. Xu and J. G. J. Verkade, *Org. Chem.*, 2003, **68**, 8416.

11 S. H. Chen, S. H. Hsiao, T. H. Su and G. S. Liou, *Macromolecules*, 2005, **38**, 307.

12 H. J. Niu, H. Q. Kang, J. W. Cai, C. Wang, X. D. Bai and W. Wang, *Polym. Chem.*, 2011, **2**, 2804.

13 R.-H. Chien, C.-T. Lai and J.-L. Hong, *J. Phys. Chem. C*, 2011, **115**, 5958.

14 Y. Hong, J. W. Y. Lam and B. Z. Tang, *Chem. Commun.*, 2009, 4332

15 (a) J. J. Stephanos, *J. Inorg. Biochem.*, 1996, **62**, 155; (b) E. Froehlich, J. S. Mandeville, C. M. Weinert, L. Kreplak and H. A. Tajmir-Riahi, *Biomacromolecules*, 2011, **12**, 511.

16 (a) J. B. LePecq and C. Paoletti, *J. Mol. Biol.*, 1967, **27**, 87; (b) A. R. Morgan and D. E. Pulleyblank, *Biochem. Biophys. Res. Commun.*, 1974, **61**, 346; (c) H. C. Birnboim and J. J. Jevcak, *Cancer Res.*, 1981, **41**, 1889.

17 Y. Liu, L. Yu, Y. Chen, Y.-L. Zhao and H. Yang, *J. Am. Chem. Soc.*, 2007, **129**, 10656.

18 (a) C. A. Sprecher, W. A. Baase and W. C. Johnson Jr, *Biopolymers*, 1979, **18**, 1009; (b) C. Zimmer and G. Luck, *Biochim. Biophys. Acta*, 1974, **361**, 11; (c) V. I. Ivanov, L. E. Minchenkova, A. K. Schyolkina and A. I. Poletayev, *Biopolymers*, 1973, **12**, 89.

19 (a) S. Hanlon, S. Brudno, T. T. Wu and B. Wolf, *Biochemistry*, 1975, **14**, 1648; (b) B. Wolf and S. Hanlon, *Biochemistry*, 1975, **14**, 1661; (c) H. S. Charles and B. C. Jonathan, *J. Am. Chem. Soc.*, 1997, **119**, 10920.

20 M. Shortreed, R. Kopelman, M. Kuhn and B. Hoyland, *Anal. Chem.*, 1996, **68**, 1414.

21 (a) S. M. Linn and R. J. Roberts, *Nucleases*, Cold Spring Harbor Labortary Press: Cold Spring Harbor, NY, 1982. (b) J. Sambrook, E. F. Fritsch, T. Maniatis, *Molecular Cloning: A Laboratory Manual*, 2nd ed., Cold Spring Harbor Laboratory Press: Cold Spring Harbor, New York, 1989.

New conjugated poly(pyridinium salt) derivative: AIE characteristics, the interaction with DNA and selective fluorescence enhancement induced by dsDNA

Ying Chang, Lu Jin, Jingjing Duan, Qiang Zhang, Jing Wang and Yan Lu*

Graphical Abstract:

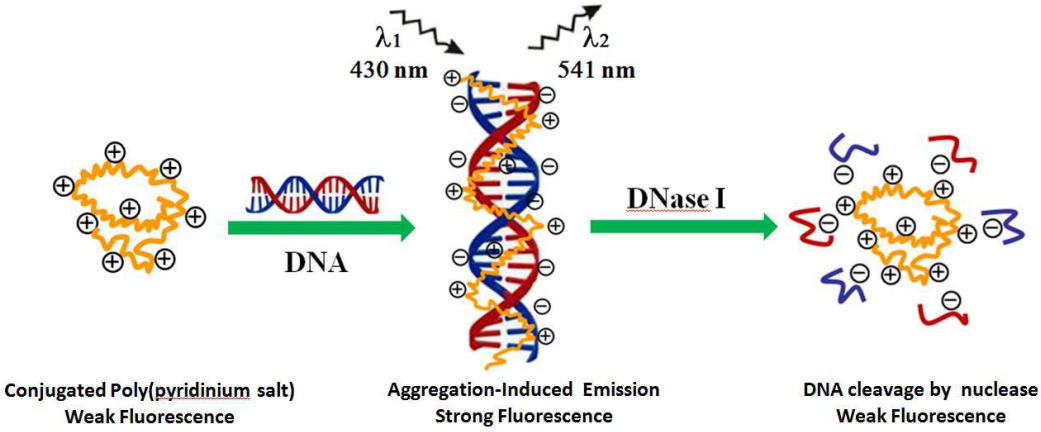

A new conjugated poly(pyridinium salt) with aggregation-induced emission characteristics was designed and synthesized for the purpose of fluorescence turn-on sensing of DNA. The probe shows excellent sensitivity and selectivity for double-stranded DNA, therefore, it was also successfully utilized to follow the DNA cleavage process by bovine pancreatic deoxyribonuclease I (DNase I).